

Study on the Variation Rule of Produced Oil Components during CO₂ Flooding in Low Permeability Reservoirs

Ganggang Hou¹, Tongjing Liu^{1,*}, Xinyu Yuan¹, Jirui Hou¹ and Pengxiang Diwu²

Abstract: CO₂ flooding has been widely studied and applied to improve oil recovery from low permeability reservoirs. Both the experimental results and the oilfield production data indicate that produced oil components (POC) will vary during CO₂ flooding in low permeability reservoirs. However, the present researches fail to explain the variation reason and rule. In this study, the physical model of the POC variation during CO₂ flooding in low permeability reservoir was established, and the variation reason and rule were defined. To verify the correctness of the physical model, the interaction rule of the oil-CO₂ system was studied by related experiments. The numerical model, including 34 components, was established based on the precise experiments matching, and simulated the POC variation during CO₂ flooding in low permeability reservoir at different inter-well reservoir characteristics. The POC monitoring data of the CO₂ flooding pilot test area in northeastern China were analyzed, and the POC variation rule during the oilfield production was obtained. The research results indicated that the existence of the inter-well channeling-path and the permeability difference between matrix and channeling-path are the main reasons for the POC variation during CO₂ flooding in low permeability reservoirs. The POC variation rules are not the same at different inter-well reservoir characteristics. For the low permeability reservoirs with homogeneous inter-well reservoir, the variation of the light hydrocarbon content in POC increases initially followed by a decrease, while the variation of the heavy hydrocarbon content in POC is completely opposite. The carbon number of the most abundant component in POC will gradually increase. For the low permeability reservoirs with the channeling-path existing in the inter-well reservoir, the variation rule of the light hydrocarbon content in POC is increase-decrease-increase-decrease, while the variation rule of the heavy hydrocarbon content in POC is completely opposite. The carbon number variation rule of the most abundant component in POC is increase-decrease-increase.

Keywords: Low permeability reservoir, CO₂ flooding, produced oil component, inter-well reservoirs characteristic.

¹ Unconventional Petroleum Research Institute, China University of Petroleum, Beijing, China.

² College of Science, China University of Petroleum, Beijing, China.

* Corresponding Author: Tongjing Liu. Email: ltjcup@cup.edu.cn.

Received: 01 November 2019; Accepted: 30 March 2020.

1 Introduction

With the exploration and development of oilfields, the proportion of low-permeability oilfields is gradually increasing [Hu, Wei and Bao (2018)]. Ensuring the development of oil in low-permeability oilfields is of great significance to the global oil supply [Asif and Muneeb (2007)]. However, low permeability reservoirs are usually characterized by multiple reservoir properties, which leads to many difficulties in development. Firstly, Due to the low permeability, it is difficult to inject water into the reservoir [Li, Zhao, Cui et al. (2008)]. Secondly, the diameter of pores and throats are great small in low permeability reservoir, resulting in huge capillary forces in the reservoir. The injected water can not sweep the small diameter pores due to the capillary forces [Wang, Zhang, Li et al. (2018)]. For that reason, CO₂ with their excellent properties has been widely used in the development of low permeability reservoirs [Qin, Han and Liu (2015); Xiao, Yang, Wang et al. (2016)].

CO₂ has the advantages of low viscosity, high mobility and small molecular size [Holm (1982); Orr, Silva, Lien et al. (1982)]. Therefore, CO₂ is easier to inject into the reservoir than water, and can sweep the tiny pores that cannot be reached by water [Grogan and Pinczewski (1987)]. CO₂ is usually in a supercritical state under reservoir temperature and pressure, which makes it have strong solubility and extraction ability [Shi, Xue and Durucan (2011)]. On the one hand, when CO₂ dissolves in oil, the viscosity of the oil decreases significantly, which will increase the oil relative permeability [Dria, Pope and Sepehrmooi (1993)]. On the other hand, CO₂ extracts the light hydrocarbons in the oil and forms a mixed phase with the oil, which can reduce the interfacial tension [Hamouda, Chukwudeme and Mirza (2009)]. Therefore, CO₂ can increase the seepage capacity of the oil phase and improve oil recovery. However, due to these characteristics of CO₂, the light hydrocarbons in oil will easily be produced, while heavy hydrocarbons in oil will be retained in the reservoir during CO₂ flooding [Gao, Zhao, Wang et al. (2014)]. For that reason, the produced oil component (POC) will vary with the CO₂ injection volume.

The results of CO₂ flooding experiments illustrate that POC will vary regardless of CO₂ miscible flooding or immiscible flooding, but the variation rules of POC are not exactly the same [Zhou, Liu, Yang et al. (2015); Cao and Gu (2013); Li, Shan, Liu et al. (2007); Darvish, Lindeberg, Holt et al. (2006)]. During CO₂ miscible flooding, the relative content of light hydrocarbons in the POC significantly increased, and the relative content of heavy hydrocarbons significantly decreased. During CO₂ immiscible flooding, the POC is the same as the initial POC before CO₂ breakthrough, but the heavy hydrocarbons in the POC increased after CO₂ breakthrough. The monitoring data of POC show that the variation of POC has the pulse characteristic during the CO₂ flooding pilot test [Diwu, Liu, You et al. (2018)]. Both the experimental data and production data indicate that the POC will vary during CO₂ flooding. However, there is not relevant research on the reasons and rules for such variation.

In this paper, we have established a physical model for the variation of POC during CO₂ flooding in low permeability by analyzing the process of CO₂ flooding. In order to verify the correctness of the physical model, firstly, related experiments have been done to measure the interaction data between oil and CO₂ under different pressure and temperature. Secondly, the experimental data have been matched using the Eclipse software, and a numerical model, including 34 components, has been established. Thirdly, CO₂ flooding is simulated at different inter-well reservoir characteristics, and the variation rule of POC is analyzed. Fourthly, based on the numerical simulation results, the production data of CO₂ flooding in the low permeability reservoir are analyzed, and then the correctness of the physical model is verified.

2 POC variation model during CO₂ flooding in low permeability reservoir

2.1 Physical model

Low permeability reservoirs have the properties of poor reservoir physical characteristics and insufficient natural energy, so that water flooding is usually used to develop the reservoir at the beginning of the reservoir development [Li (1998); Liu and Li (2012); Wang, Liao and Zhao (2014)]. During the oilfield development, it is easy to form the channeling-path between parts of the injection well and production well because of the strong stress sensitivity and wide distribution of natural fracture in low permeability reservoirs [Ruan and Wang (2002)]. Therefore, some inter-well reservoir are relatively homogeneous, others have the channeling-path during the development of low permeability reservoirs. Due to the low permeability of the matrix, the permeability will have a large level difference between the matrix and channeling-path when the inter-well reservoir has the channeling-path [Wang, Wang, Chen et al. (2010)]. The seepage velocity of CO₂ in the matrix is less than in channeling-path after CO₂ is injected. Therefore, the variation rule of POC is not exactly same at different inter-well reservoir conditions during CO₂ flooding.

For the low permeability reservoirs with homogeneous inter-well reservoir, the variation rules of POC are mainly divided into three stages during CO₂ flooding, as shown in Fig. 1. In the first stage, CO₂ is injected as a displacement phase to displace oil to the production well, as shown in Fig. 1(a). At this stage, the produced oil does not contact with CO₂, and the POC is the same as the end of water flooding. The most abundant component in POC is the same as the end of water flooding. In the second stage, the produced oil mainly comes from the flooding front formed by CO₂ extracting the light hydrocarbons in crude oil, as shown in Fig. 1(b). The content of light hydrocarbons is relatively high in the flooding front, so that light hydrocarbons in the POC will increase, and heavy hydrocarbons in the POC will decrease. The carbon number of the most abundant component in POC will stay the same or decrease. In the third stage, the remaining oil is produced, which come from the CO₂ flushing the oil in the pores and throats, as shown in Fig. 1(c). The content of heavy hydrocarbons is relatively high in the remaining oil, so that light hydrocarbons in the POC will decrease, and heavy

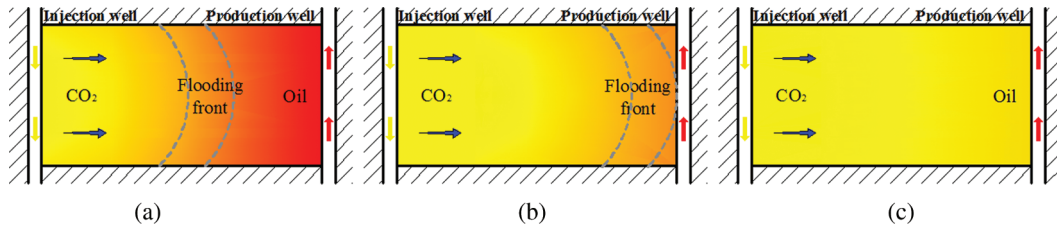


Figure 1: Schematic diagram of CO₂ flooding in low permeability reservoirs with homogeneous inter-well reservoir. (a) Stage I. (b) Stage II. (c) Stage III

hydrocarbons in the POC will increase. The carbon number of the most abundant component in POC will gradually increase.

For the low permeability reservoirs with the channeling-path existing in the inter-well reservoir, after CO₂ injection, some of them displace the oil in channeling-path, and others displace the oil in the matrix. Due to the permeability difference between the matrix and channeling-path in low permeability reservoirs, the oil in channeling-path will preferentially be produced than the oil in the matrix. The interaction rules of the oil-CO₂ system are always the same whether in the matrix or in the channeling-path. Therefore, according to the order of oil being produced and the interaction rules of the oil-CO₂ system, the CO₂ flooding process is divided into two parts and six stages in the low permeability reservoir with inter-well channeling-path existed, as shown in Fig. 2.

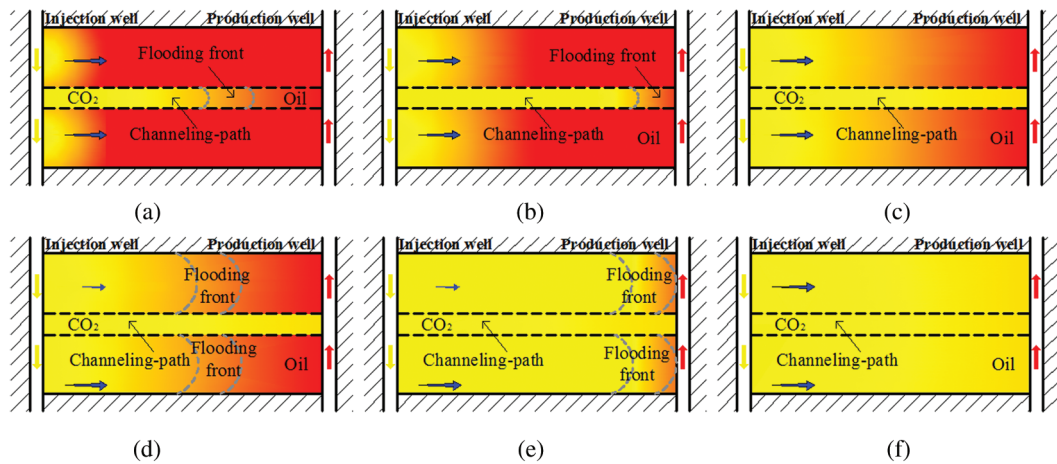


Figure 2: Schematic diagram of CO₂ flooding in low permeability reservoirs with the channeling-path existing in the inter-well reservoir. (a) Stage I of the first part. (b) Stage II of the first part. (c) Stage III of the first part. (d) Stage I of the second part. (e) Stage II of the second part. (f) Stage III of the second part

In the first part, the oil in channeling-path displaced by CO₂ is produced. In the first stage, the produced oil mainly comes from the channeling-path and does not contact with CO₂, as shown in Fig. 2(a). So the POC is the same as the ending of water flooding. The most abundant component in POC is the same as the end of water flooding. In the second stage, the produced oil mainly comes from the flooding front that formed by CO₂ exacting the light hydrocarbons in channeling-path, as shown in Fig. 2(b). The content of light hydrocarbons is relatively high in the flooding front, so that light hydrocarbons in the POC will increase, and heavy hydrocarbons in the POC will decrease. The carbon number of the most abundant component in POC will stay the same or decrease. In the third stage, the remaining oil is produced, which come from the CO₂ flushing the oil in the channeling-path, as shown in Fig. 2(c). The content of heavy hydrocarbons is relatively high in the remaining oil, so that light hydrocarbons in the POC will decrease, and heavy hydrocarbons in the POC will increase. The carbon number of the most abundant component in POC will gradually increase.

In the second part, the oil in the matrix displaced by CO₂ is produced. In the first stage, the produced oil mainly comes from the matrix and does not contact with CO₂, as shown in Fig. 2(d). So the POC is the same as the ending of water flooding. The most abundant component in POC is the same as the end of water flooding. In the second stage, the produced oil mainly comes from the flooding front that formed by CO₂ exacting the light hydrocarbons in the matrix, as shown in Fig. 2(e). The content of light hydrocarbons is relatively high in the flooding front, so that light hydrocarbons in the POC will increase, and heavy hydrocarbons in the POC will decrease. The carbon number of the most abundant component in POC will stay the same or decrease. In the third stage, the remaining oil is produced, which come from the CO₂ flushing the oil in the matrix, as shown in Fig. 2(f). The content of heavy hydrocarbons is relatively high in the remaining oil, so that light hydrocarbons in the POC will decrease, and heavy hydrocarbons in the POC will increase. The carbon number of the most abundant component in POC will gradually increase.

In summary, the variation rule of POC is not exactly same at different inter-well reservoir conditions during CO₂ flooding in low permeability reservoir. For the low permeability reservoirs with homogeneous inter-well reservoir, the variation of the light hydrocarbon content in POC increases initially followed by a decrease, while the variation of the heavy hydrocarbon content in POC is completely opposite. The carbon number of most abundant component in POC will gradually increase. For the low permeability reservoirs with the channeling-path existing in the inter-well reservoir, the variation rule of the light hydrocarbon content in POC is increase-decrease-increase-decrease, while the variation rule of the heavy hydrocarbon content in POC is completely opposite. The carbon number variation rule of most abundant component in POC is increase-decrease-increase. In order to verify the correctness of the physical model, relevant experiments have been done, and the component numerical models have been established to analyze the variation rules of POC during CO₂ flooding in low permeability reservoir.

2.2 Mathematical model

During CO₂ flooding, a mixture of gas and liquid is produced. The POC variation is the same as the variation of the molar fraction of hydrocarbon components in the liquid phase. Therefore, the primary target of the mathematical models is to calculate the molar fraction of hydrocarbon components in the liquid phase.

It is assumed that the total mass of the mixture produced by the oil well is N_F . So, at any time, the molar fractions of the liquid phase and gas phase in the mixture must sum up to N_F . The equation can be expressed as:

$$N_l + N_g = N_F \quad (1)$$

where N_l and N_g is the molar fraction of liquid phase and gas phase in the mixture.

The material balance equation of component i can be written as:

$$N_l x_i + N_g y_i = N_F z_i \quad (2)$$

where x_i , y_i and z_i is the molar fraction of component i in liquid phase, gas phase and mixture phase, respectively.

The equilibrium constant K_i and gasification rate v is introduced. The calculation formulas is written as:

$$K_i = \frac{y_i}{x_i} \quad (3)$$

$$v = \frac{N_g}{N_F} \quad (4)$$

Therefore, the x_i , y_i can be written as:

$$x_i = \frac{z_i}{1 + v(K_i - 1)} \quad (5)$$

$$y_i = \frac{K_i z_i}{1 + v(K_i - 1)} \quad (6)$$

The molar fractions of component i in each phase must sum up to one which can be written as:

$$\sum_i^N x_i = \sum_i^N \frac{z_i}{1 + v(K_i - 1)} = 1 \quad (7)$$

$$\sum_i^N y_i = \sum_i^N \frac{K_i z_i}{1 + v(K_i - 1)} = 1 \quad (8)$$

from which:

$$f = \sum_i^N (y_i - x_i) = \sum_i^N \frac{z_i(K_i - 1)}{1 + v(K_i - 1)} = 0 \quad (9)$$

According to the phase equilibrium equation, the K_i also can be expressed as:

$$K_i = \frac{\phi_i^l}{\phi_i^g} \quad (10)$$

where ϕ_i^l and ϕ_i^g is the fugacity coefficient of component i in the liquid phase and gas phase. The ϕ_i^l and ϕ_i^g vary with pressure (P) and temperature (T), and it can be calculated by the equation of state (EOS). Derivation of Eq. (6) can be written as follows:

$$\frac{df}{dv} = - \sum_i^N \frac{z_i(K_i - 1)^2}{(1 + v(K_i - 1))^2} \quad (11)$$

At some point in oilfield production, the P , T , N_F and z_i are given parameters. The mole fraction of hydrocarbon components in the liquid phase can be obtained by using the Newton's method. The general formula for the k -th iteration is:

$$f(v_k) + \left[\frac{df(v)}{d(v)} \right]_{v=v_k} (v_{k+1} - v_k) = 0 \quad (12)$$

$$v_{k+1} = v_k - \frac{f(v_k)}{f'(v_{k+1})} \quad (13)$$

A simple flow chart of calculating x_i and y_i is shown in Fig. 3.

3 Experimental section

3.1 Materials

In this study, the oil sample from northeast China was applied to measure the phase behaviors of oil-CO₂ systems. The properties of dead oil and live oil are shown in Tab. 1, and the compositional analysis of the oil samples under the reservoir conditions (23.21 MPa, 97.3°C) is listed in Tab. 2. The minimum miscibility pressure (MMP) of the live oil sample was measured using a traditional slim tube, and the MMP measured as 22.1 MPa [Ma, Wang, Gao et al. (2016)]. The purities of CO₂ and N₂ (leakage-free test gas) were 99% and 99.9%, respectively.

3.2 Experimental setup

In the experimental studies, CO₂ was recombined into a reservoir oil sample to generate light oil-CO₂ systems under different pressures for measuring phase behaviors. A plunger type PVT system (210/1500 FV, ST, French) was used to measure the properties of the

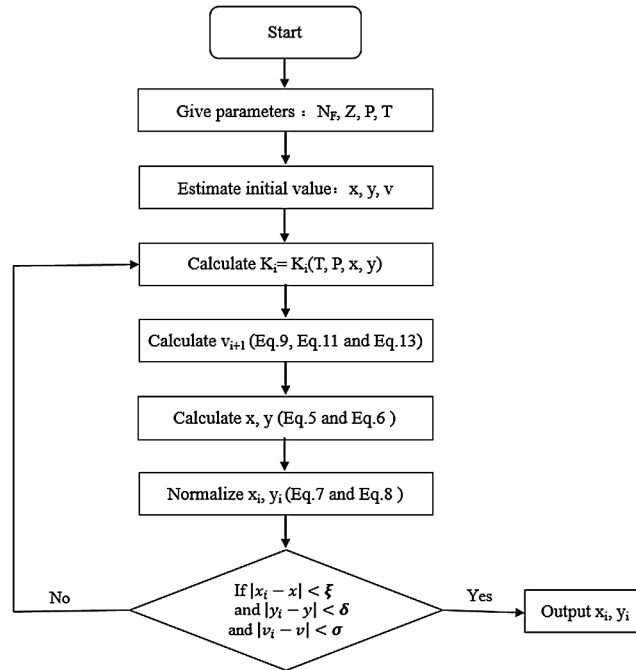


Figure 3: Flow chart of calculating x_i and y_i

Table 1: Properties of the dead oil and live oil

Parameter	Dead oil	Live oil
Crude oil viscosity (mPa·s)	3.19	1.85
Crude oil density (kg/m ³)	850.3	761.5
Solution gas-oil ratio (GOR) (Sm ³ /m ³)	/	36.7
Saturation pressure (MPa)	/	7.01
Oil formation volume factor (m ³ /m ³)	/	1.2

Note: The properties of dead oil were measured under atmosphere conditions, while the properties of live oil were tested under reservoir conditions (23.1 MPa, 97.3°C).

oil-CO₂ system, as shown in Fig. 4. The PVT system is mainly composed of PVT test chamber, constant temperature air bath, pressure and temperature sensor, metering pump and operating system. The PVT test chamber is located in the constant temperature air bath, in which the temperature is controlled by temperature sensor and operating system. A plunger pump is connected to the PVT system to control the pressure of the PVT test chamber. The effective volume of the PVT test chamber is 240 ml and the highest pressure and temperature it can withstand is 150 MPa and 200°C, respectively. In

Table 2: Compositional analysis results of the oil sample

Composition	MD (mol%)	SD (mol%)	Composition	MD (mol%)	SD (mol%)
CO ₂	0.343	0.35	C ₁₆	2.325	2.31
N ₂	1.971	1.87	C ₁₇	2.323	2.32
C ₁	16.739	16.72	C ₁₈	2.17	2.2
C ₂	5.901	5.91	C ₁₉	1.962	1.95
C ₃	3.843	3.85	C ₂₀	1.877	1.88
C ₄	1.696	1.74	C ₂₁	1.773	1.76
C ₅	2.373	2.43	C ₂₂	1.598	1.56
C ₆	1.576	1.59	C ₂₃	1.533	1.52
C ₇	2.253	2.28	C ₂₄	1.438	1.42
C ₈	5.319	5.35	C ₂₅	1.271	1.26
C ₉	5.349	5.39	C ₂₆	1.198	1.18
C ₁₀	4.264	4.28	C ₂₇	1.161	1.15
C ₁₁	3.663	3.78	C ₂₈	1.053	1.03
C ₁₂	3.71	3.77	C ₂₉	0.963	0.96
C ₁₃	3.167	3.39	C ₃₀	0.93	0.93
C ₁₄	2.676	2.65	C ₃₁	0.75	0.75
C ₁₅	2.881	2.85	C ₃₁₊	7.951	7.62

Note: MD=measured data; SD=simulation data.

addition to the PVT system, the experimental equipment also includes a vacuum pump, intermediate container, and other measuring equipment.

3.3 Experimental procedures

In order to measure the phase behavior of oil-CO₂ system under different pressures, the main experimental steps are summarized as follows:

1. Prior to fluid injection, clean the PVT test chamber and vacuum it using the vacuum pump. Then, inject the testing oil sample to the PVT test chamber and set the temperature of the air bath to the target temperature for 24 h to ensure that the temperature of oil sample reached the target temperature.
2. The designed volume of CO₂ is injected into the PVT test chamber to form the oil-CO₂ system, and make sure the system in an equilibrium status under designed pressure and temperature conditions.
3. Measure the saturation pressure, swelling factor, solution gas-oil ratio, density and viscosity of the oil-CO₂ system.

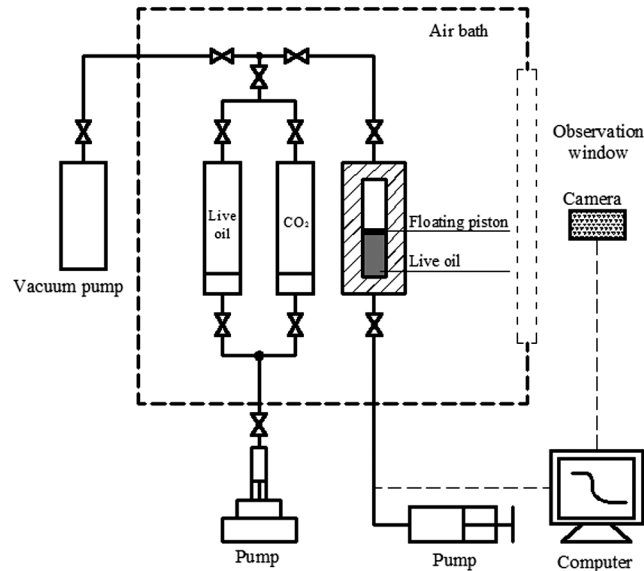


Figure 4: Schematic of the experimental setup for the PVT tests of oil-CO₂ system

4 Numerical simulation

4.1 Phase behavior matching study

To establish an accurate numerical model, it is necessary to match the PVT data of the oil-CO₂ system measured from the experiments and gain the necessary parameters for establishing the numerical model. Prior to phase behavior matching, the oil components should be divided according to the research.

In this study, the PVTi module of the Eclipse software was used to match the experimental data. The Soave-Redlich-Kwong (SRK) equation of state was used to compute the saturation pressure, oil swelling factor, density, and viscosity of the light oil-CO₂ system with different CO₂ concentrations. The SRK equation can be written as:

$$P = RT / (V - b) - a_c \alpha / [V(V + b)] \quad (14)$$

$$a_c = 0.42747R^2 T_c / P_c \quad (15)$$

$$b = 0.08664RT_c / P_c \quad (16)$$

$$\alpha = [1 + m(1 - T_r^{0.5})]^2 \quad (17)$$

$$m = 0.048 + 1.574\omega - 0.176\omega^2 \quad (18)$$

where P is the pressure, R is ideal gas constant, T is the absolute temperature, V is the volume, T_c is absolute temperature at the critical point, P_c is pressure at the critical point, T_r is the reduced temperature, ω is the acentric factor for the species.

In order to accurately analyze the variation rules of POC during CO₂ flooding, 34 components were used to match the phase behavior, as shown in Tab. 2. The reservoir temperature, reservoir pressure and saturation pressure was set to 88°C, 22.5 MPa and 7.01 MPa, respectively.

The measured and simulated saturation pressures and oil swelling factor were shown in Fig. 5. The measured and simulated density and the viscosity of the light oil-CO₂ system were tabulated in Tabs. 3 and 4, respectively. The errors were calculated using Eq. (19):

$$Error = \frac{|MD - SD|}{MD} \times 100\% \quad (19)$$

Fig. 5, Tabs. 3 and 4 indicate that the simulation data are close to the measurement. The maximum errors for the density and viscosity are 3.197% and 3.388%, respectively. Thus, the simulation results are acceptable.

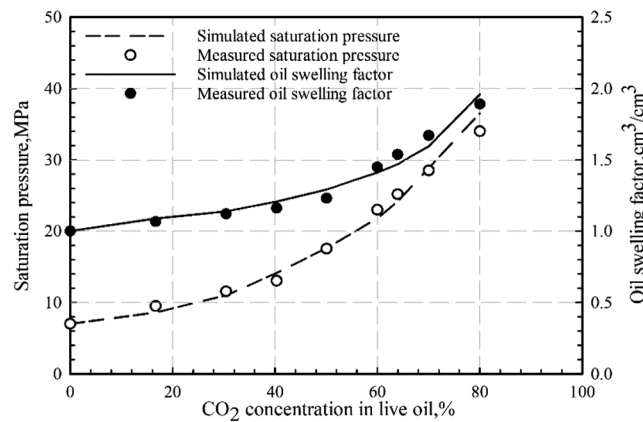


Figure 5: Measured and simulated saturation pressures and oil swelling factor for light oil-CO₂ systems with different CO₂ concentrations

4.2 Multi-component mathematical model

In this work, an isothermal compositional multiphase fluid flow in porous media is considered. The assumptions of the multi-component mathematical model are presented as follow:

1. Isothermal reservoir rock, fluid, and injecting fluids.
2. Local phase equilibrium.
3. Three phases and N components in the reservoir.
4. Phase velocities evaluated through the modified Darcy's law.
5. No hydrocarbon dissolution or solubilization into the aqueous phase.

Table 3: Densities of the light oil-CO₂ system with different CO₂ concentrations under different pressures

C _{CO₂}	P(MPa): 24.2			P(MPa): 7.01		
	MD (g/cm ³)	SD (g/cm ³)	Error (%)	MD (g/cm ³)	SD (g/cm ³)	Error (%)
0.00	0.7615	0.7414	2.6395	0.7453	0.7521	0.912384
16.68	0.7701	0.7632	0.8962	0.7492	0.7612	1.597354
30.43	0.7756	0.7743	0.1682	0.7564	0.7763	2.633003
40.32	0.7662	0.7721	0.7741	0.7508	0.7615	1.426968
50.05	0.7607	0.7652	0.0696	0.7493	0.7391	1.367835
63.96	0.7580	0.7631	0.2770	0.7580	0.7553	0.356201

Note: C_{CO₂}=concentration of CO₂ in light oil-CO₂ systems; P=pressure; MD=measured data; SD=simulation data.

Table 4: Viscosities of the light oil-CO₂ system with different CO₂ concentrations under different pressures

C _{CO₂}	P(MPa): 24.2			P(MPa): 7.01		
	MD (mPa.s)	SD (mPa.s)	Error (%)	MD (mPa.s)	SD (mPa.s)	Error (%)
0.00	1.85	1.8300	1.0811	1.47	1.45	1.360544
16.68	1.42	1.4100	0.7042	1.18	1.21	2.542373
30.43	1.11	1.1500	3.3243	0.99	1.03	4.040404
40.32	0.95	0.9900	4.2105	0.87	0.89	2.890173
50.05	0.82	0.8400	2.4390	0.78	0.81	3.846154
63.96	0.68	0.7100	4.4118	0.68	0.71	4.411765

Note: C_{CO₂}=concentration of CO₂ in light oil-CO₂ systems; P=pressure; MD=measured data; SD=simulation data.

The material balance equation of component *i* can be written as:

$$\begin{aligned}
 & -\vec{\nabla} \cdot [C_{io}\rho_o \vec{v}_o + C_{ig}\rho_g \vec{v}_g + C_{iw}\rho_w \vec{v}_w] + q_i \\
 & = \frac{\partial}{\partial t} [\phi(C_{io}\rho_o S_o + C_{ig}\rho_g S_g + C_{iw}\rho_w S_w)] \quad i=1, \dots, N
 \end{aligned} \tag{20}$$

where C_{io} , C_{iw} and C_{ig} are the molar fraction of component *i* in phase oil, water and gas, respectively, ρ_o , ρ_w and ρ_g are the density of oil, water and gas phase, respectively, q_i is the molar flow rate of component *i* due to well injection/production per unit of bulk volume, S_o , S_w and S_g are the saturation of oil, water and gas phase, respectively, ϕ is the porosity, $\vec{\nabla}$ is the Hamiltonian, and it can be written as:

$$\vec{\nabla} = \frac{\partial}{\partial x} i + \frac{\partial}{\partial y} j + \frac{\partial}{\partial z} k \quad (21)$$

The Darcy's formula considering gravity action is as follows:

$$\begin{cases} \vec{v}_g = -\frac{\bar{K}k_{rg}}{\mu_g} (\vec{\nabla}P_g - \rho_g g \vec{\nabla}D) \\ \vec{v}_o = -\frac{\bar{K}k_{ro}}{\mu_o} (\vec{\nabla}P_o - \rho_o g \vec{\nabla}D) \\ \vec{v}_w = -\frac{\bar{K}k_{rw}}{\mu_w} (\vec{\nabla}P_w - \rho_w g \vec{\nabla}D) \end{cases} \quad (22)$$

where \bar{K} is the absolute permeability tensor, k_{ro} , k_{rw} and k_{rg} are the relative permeability of oil, water and gas phase, respectively, μ_o , μ_w and μ_g are the viscosity of oil, water and gas phase, respectively, P_o , P_w and P_g are the pressure of oil, water and gas phase, respectively, g is the gravity acceleration, D is the depth.

Combing the Eqs. (20) and (22), the material balance equation of component i can be written as:

$$\begin{aligned} & \vec{\nabla} \cdot \left[\frac{C_{io}\rho_o\bar{K}k_{ro}}{\mu_o} (\vec{\nabla}P_o - \rho_o g \vec{\nabla}D) + \frac{C_{ig}\rho_g\bar{K}k_{rg}}{\mu_g} (\vec{\nabla}P_g - \rho_g g \vec{\nabla}D) \right. \\ & \left. + \frac{C_{iw}\rho_w\bar{K}k_{rw}}{\mu_w} (\vec{\nabla}P_w - \rho_w g \vec{\nabla}D) \right] + q_i \\ & = \frac{\partial}{\partial t} [\phi(C_{io}\rho_o S_o + C_{ig}\rho_g S_g + C_{iw}\rho_w S_w)] \quad i=1, \dots, N \end{aligned} \quad (23)$$

The fluid saturation in the reservoir must sum up to one. The equation can be expressed as:

$$S_o + S_g + S_w = 1 \quad (24)$$

The molar mass of each phase must sum up to one which is given by:

$$\sum_{i=1}^N C_{io} = 1 \quad (25)$$

$$\sum_{i=1}^N C_{iw} = 1 \quad (26)$$

$$\sum_{i=1}^N C_{ig} = 1 \quad (27)$$

The relationship of capillary force in the reservoir is written as:

$$p_{cgo} = p_g - p_o \quad (28)$$

$$p_{cow} = p_o - p_w \quad (29)$$

The equilibrium constant of component i is written as:

$$\frac{C_{ig}}{C_{io}} = k_{igo}(T, p_g, p_o, C_{ig}, C_{io}) \quad (30)$$

$$\frac{C_{ig}}{C_{iw}} = k_{igw}(T, p_g, p_w, C_{ig}, C_{iw}) \quad (31)$$

where k_{igo} are the equilibrium constant of component i in phase oil and gas, k_{igw} are the equilibrium constant of component i in phase water and gas.

The boundary conditions of the model including outer boundary condition and inner boundary condition. The outer boundary condition can be written as:

$$P|_{r=r_e} = const \quad (32)$$

The inner boundary condition can be written as:

$$q|_{r=r_w} = const \quad (33)$$

where r_e is the radius of reservoir, r_w is the radius of well. In this work, In order to obtain higher calculation speed, the adaptive implicit methods was been used, which obtained by combining a Fully Implicit (FI) formulation with an IMPES approach.

4.3 Numerical model establishment

In order to study the variation rule of POC during CO₂ flooding in low permeability reservoirs, a typical numerical model was established using the E300 module of Eclipse software. There were 5 wells in the model, of which 4 production wells (P1-well, P2-well, P3-well, and P4-well) located around the model, and 1 injection well (I1-well) located in the middle of the model. In the numerical model, 19,19,11 grids were developed in the i,j,k direction, and the size of the model in each direction are 570 m, 570 m, and 6.6 m, respectively, as shown in Fig. 6. The model properties (saturation and porosity) and initial conditions (temperature and pressure) are the same as the oilfield in northeastern China, as shown in Tab. 5.

The physical model proposed a hypothesis that the POC variation rule was not the same at different inter-well reservoir characteristics during CO₂ flooding in low permeability reservoirs. In order to verify the correctness of the hypothesis, two types of the numerical model were established, which were the numerical model with homogeneous inter-well reservoir and the numerical model with channeling-path existing in the inter-well

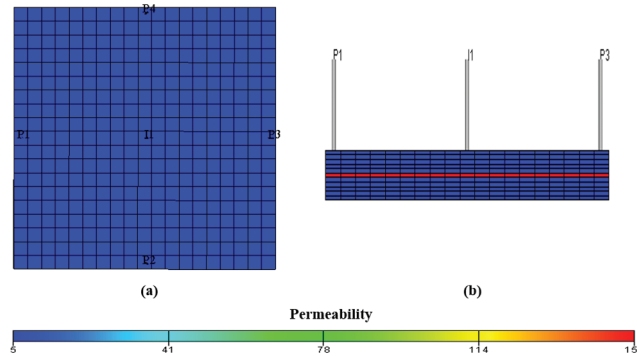


Figure 6: Schematic of the numerical model at different inter-well reservoir characteristics: (a) Front view of homogeneous inter-well reservoir; (b) Section view of channeling-path existing in the inter-well reservoir

Table 5: Parameters setting in the numerical model

Parameter	Value	Parameter	Value
Initial formation pressure	22.5 MPa	Initial formation temperature	88°C
Initial oil saturation	0.549	Formation porosity	0.12

reservoir. For the numerical model with homogeneous inter-well reservoir, the permeability was 5 mD. The front view of the model was shown in Fig. 6(a). For the numerical model with channeling-path existing in the inter-well reservoir, the channeling-path located between the P1-well and the P3-well in the plane and the 6th layer in the vertical direction. The permeability of the matrix and channeling-path was 5 mD and 150 mD, respectively. The Section view of the model was shown as Fig. 6(b).

For simulating the oilfield production status, the numerical model applied CO₂ flooding after water flooding. During CO₂ flooding the injection well continuously injected the gas and the simulation finished when the cumulative gas injection amount was 1 PV. In the numerical model, the oil production rate was 10 sm³/d, the water injection rate was 40 sm³/d, and the gas injection rate was 8000 sm³/d.

4.4 Simulation results and analysis

C₁-C₄ in the oil components is gaseous under the atmosphere conditions. According to the setting of the components in the numerical model, the variation of C₅-C₃₁ in the POC will be analyzed to determine the POC variation rules during CO₂ flooding. The ability of CO₂ extraction C₅-C₁₅ from oil is significantly stronger than the ability of CO₂ extraction C₁₆-C₃₁₊ from oil [Hu, Hao, Chen et al. (2019)]. So the relative content variation of C₅-C₁₅ and C₁₆-C₃₁₊ in the POC will be analyzed separately. The numerical model, including 34 components, was used to simulate the CO₂ flooding in low permeability reservoir at

different inter-well reservoir condition, and the POC variation rules was analyzed. The simulation results were as follows.

For the low permeability reservoirs with homogeneous inter-well reservoir, the simulation results were shown in Figs. 7 and 8. At the end of water flooding, that is, the CO₂ injection amount is 0 PV. The relative content of C₅-C₁₅ in the POC is less than the relative content of C₁₆-C₃₁₊, and the most abundant component in the POC is C₉. When the CO₂ injection amount is 0.1 PV, the relative content of C₅-C₁₅ in the POC increase, and the relative content of C₁₆-C₃₁₊ decrease. The most abundant component in the POC is C₉. When the CO₂ injection amount is 0.5PV, the relative content of C₅-C₁₅ in the POC decrease, and the relative content of C₁₆-C₃₁₊ increase. The most abundant component in the POC changes from C₉ to C₁₂. When the CO₂ injection amount is 1PV, the relative content of C₅-C₁₅ in the POC decrease, and the relative content of C₁₆-C₃₁₊ increase. The most abundant component in the POC changes from C₁₂ to C₁₅.

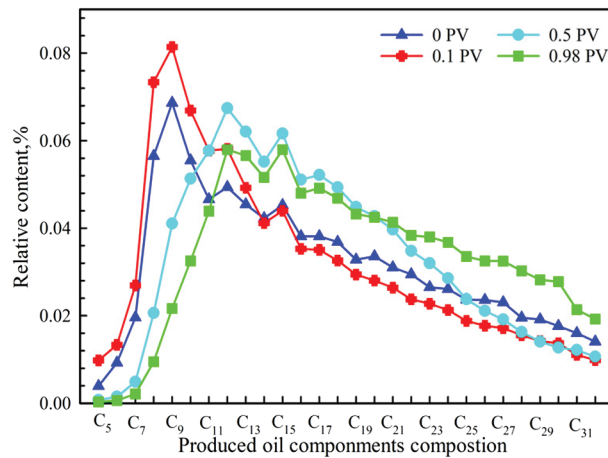


Figure 7: POC variation in the numerical model with homogeneous inter-well reservoir during CO₂ flooding

For the low permeability reservoirs with the channeling-path existing in the inter-well reservoir, the simulation results were shown in Figs. 9 and 10. At the end of water flooding, that is, the CO₂ injection amount is 0 PV. The relative content of C₅-C₁₅ in the POC is more than the relative content of C₁₆-C₃₁₊, and the most abundant component in the POC is C₉. When the CO₂ injection amount is 0.003 PV, the relative content of C₅-C₁₅ in the POC increase, and the relative content of C₁₆-C₃₁₊ decrease, and the most abundant component in the POC is C₉. When the CO₂ injection amount is 0.031 PV, the relative content of C₅-C₁₅ in the POC decrease, and the relative content of C₁₆-C₃₁₊ increase, and the most abundant component in the POC changes from C₉ to C₃₀. When the CO₂ injection amount is 0.4 PV, the relative content of C₅-C₁₅ in the POC increase, and the relative content of C₁₆-C₃₁₊ decrease, and the most abundant component in the

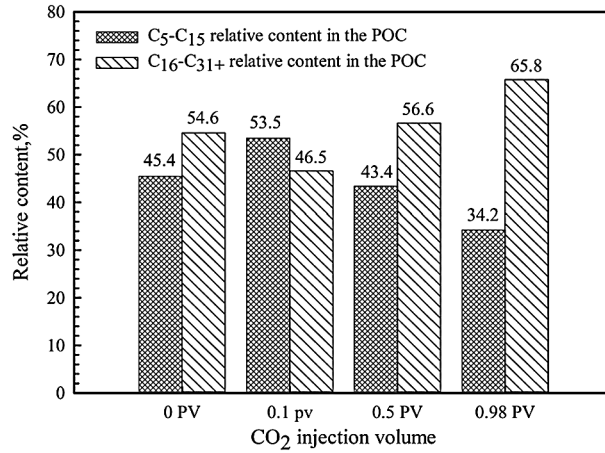


Figure 8: C₅-C₁₅ and C₁₆-C₃₁₊ relative content in numerical model with homogeneous inter-well reservoir during CO₂ flooding

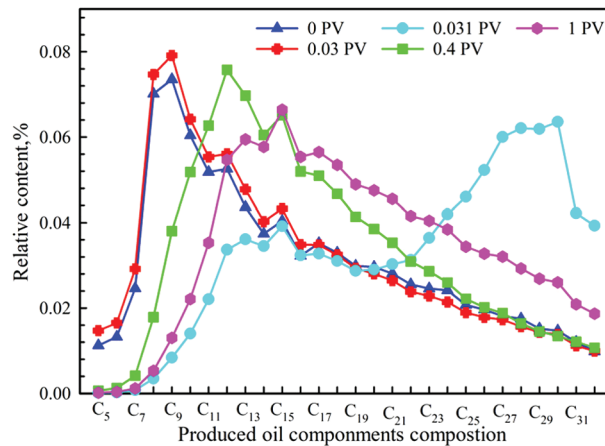


Figure 9: POC variation in the numerical model with channeling-path existing in the inter-well reservoir during CO₂ flooding

POC changes from C₃₀ to C₁₂. When the CO₂ injection amount is 1PV, the relative content of C₅-C₁₅ in the POC decrease, and the relative content of C₁₆-C₃₁₊ increase, and the most abundant component in the POC changes from C₁₂ to C₁₅.

In summary, the simulation results indicate that for the low permeability reservoirs with homogeneous inter-well reservoir, the variation of the light hydrocarbon relative content in POC increases initially followed by a decrease, while the variation of the heavy hydrocarbon relative content in POC is completely opposite. The carbon number of the most abundant component in POC will gradually increase (C₉-C₁₂-C₁₅). For the low

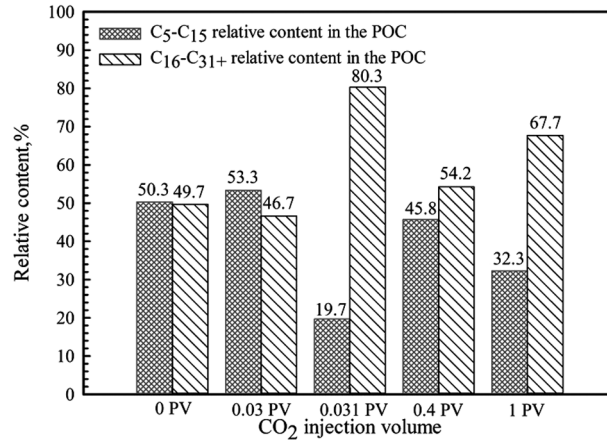


Figure 10: C₅-C₁₅ and C₁₆-C₃₁₊ relative content in the numerical model with channeling-path existing in the inter-well reservoir during CO₂ flooding

permeability reservoirs with the channeling-path existing in the inter-well reservoir, the variation of the light hydrocarbon relative content in POC is an increase-decrease-increase-decrease, while the variation of the heavy hydrocarbon relative content in POC is completely opposite. The carbon number variation of most abundant component in POC is an increase-decrease-increase (C₉-C₃₀-C₁₂-C₁₅).

The numerical simulation results are the same as the conclusions of the physical model hypothesis, so the numerical model verifies the correctness of the physical model. In order to further verify the correctness of the physical model during the oilfield production, the POC monitoring data will be analyzed, which get from a CO₂ flooding pilot test area of low permeability reservoir in northeastern China.

5 Analysis of the oilfield production data

In May 2008, a pilot test area of low permeability reservoir in northeastern China applied CO₂ flooding to enhance the oil recovery. There are 6 injection wells and 27 production wells in the pilot test area. The reservoir characteristic parameters such as initial formation pressure, temperature, permeability, and viscosity are 24.3 MPa, 98.9°C, 3.57 mD and 1.85 mPa·s respectively. The MMP of the live oil is 21.5 MPa.

In order to monitor the time of gas breakthrough and the variation rules of POC during CO₂ flooding in the pilot test area, the produced oil and gas components are tested for all production wells. The POC variation rule can be divided into two types by analyzing the POC monitoring data. Take the POC monitoring data and the CO₂ content monitoring data of P1-well and P2-well as examples to analyze the variation rule of the two types.

In September 2007, the P1-well began to produce oil. The injection well that provided the CO₂ for P1-well began to inject gas in March 2009, and the gas injection rate was 7000 m³/d. As of February 2013, the POC of P1-well was tested four times. The tested results were shown

in Fig. 11. The relative content variation of C₅-C₁₅ and C₁₆-C₃₁₊ were shown in Fig. 12. In March 2009, the relative content of C₅-C₁₅ in the POC was more than the relative content of C₁₆-C₃₁₊, and the most abundant component in POC was C₈. In February 2010, the relative content of C₅-C₁₅ in the POC decreased, and the relative content of C₁₆-C₃₁₊ increased. The most abundant component in POC was C₈. In June 2011, the relative content of C₅-C₁₅ in the POC decreased, and the relative content of C₁₆-C₃₁₊ increased. The most abundant component in POC changed from C₈ to C₁₀. In February 2013, the relative content of C₅-C₁₅ in the POC decreased, and the relative content of C₁₆-C₃₁₊ increased. The most abundant component in POC changed from C₁₀ to C₁₈.

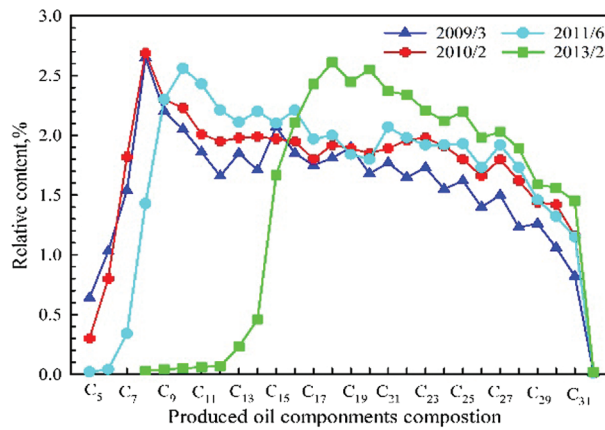


Figure 11: The POC monitoring data of P1-well in CO₂ flooding pilot test area

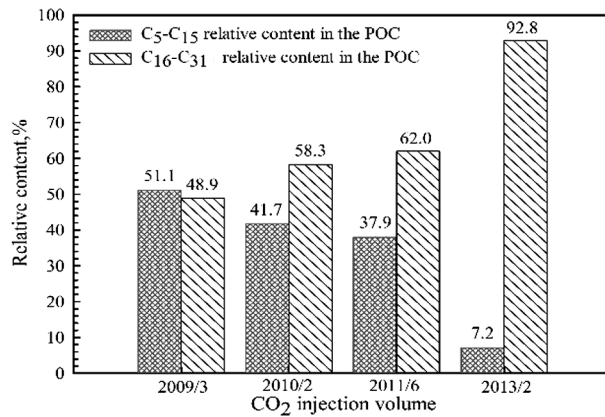


Figure 12: C₅-C₁₅ and C₁₆-C₃₁₊ relative content of P1-well in CO₂ flooding pilot test area

In September 2007, the P2-well began to produce oil. The injection well that provided the CO₂ for P2-well began to inject gas on March 2009, and the gas injection rate was 6700 m³/d. As of February 2013, the POC of P2-well was tested four times. The tested results were shown in Fig. 13. The relative content variation of C₅-C₁₅ and C₁₆-C₃₁₊ were shown in Fig. 14. In March 2009, the relative content of C₅-C₁₅ in the POC was less than the relative content of C₁₆-C₃₁₊, and the most abundant component in POC was C₈. In September 2011, the relative content of C₅-C₁₅ in the POC decreased, and the relative content of C₁₆-C₃₁₊ increased. The most abundant component in POC changed from C₈ to C₁₅. In August 2012, the relative content of C₅-C₁₅ in the POC increased, and the relative content of C₁₆-C₃₁₊ decreased. The most abundant component in POC changed from C₁₅ to C₈. In February 2013, the relative content of C₅-C₁₅ in the POC decreased, and the relative content of C₁₆-C₃₁₊ increased. The most abundant component in POC changed from C₈ to C₁₃.

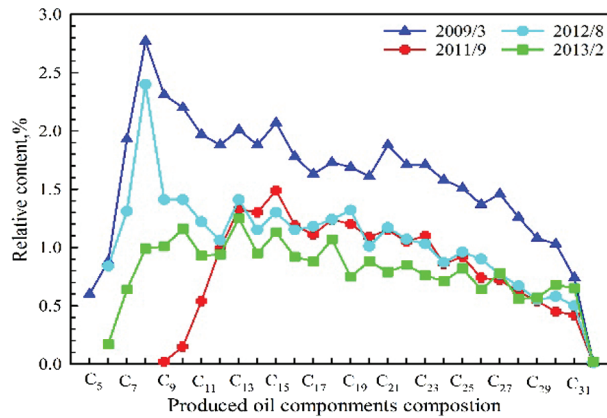


Figure 13: The POC monitoring data of P2-well in CO₂ flooding pilot test area

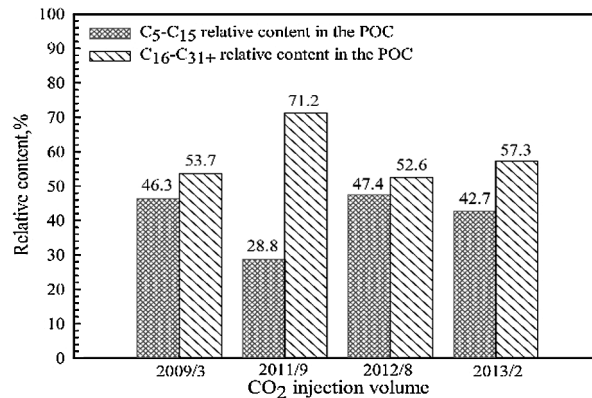


Figure 14: C₅-C₁₅ and C₁₆-C₃₁₊ relative content of P2-well in CO₂ flooding pilot test area

The relative content of CO₂ in the produced gas was monitored during the production of P1-well and P2-well. The results were shown in Fig. 15. The monitoring data indicate that the CO₂ breakthrough time for P1-well and P2-well is November 2011 and September 2009, respectively. So that, for the P1-well and the P2-well, the gas breakthrough occurred at 43 months and 6 months after CO₂ injection. It indicates that the reservoir between the P1-well and its corresponding injection well is relatively homogeneous, and the reservoir between the P2-well and its corresponding injection well exist the channeling-path.

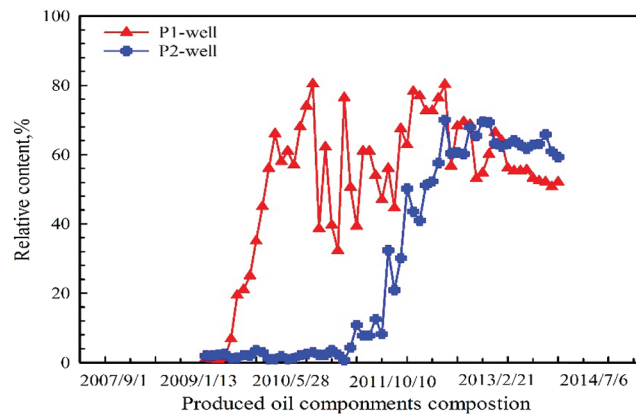


Figure 15: CO₂ concentration date of P1-well and P2-wells

In summary, for the low permeability reservoirs with homogeneous inter-well reservoir (P1-well), the light hydrocarbons in the POC will decrease, and heavy hydrocarbons in the POC will increase. The carbon number of the most abundant component in POC will increase. For the low permeability reservoirs with the channeling-path existing in the inter-well reservoir (P2-well), the variation rule of the light hydrocarbon content in POC is a decrease-increase-decrease, while the variation rule of the heavy hydrocarbon content in POC is completely opposite. The variation rule of carbon number of most abundant component in POC is an increase-decrease-increase.

Comparing the variation rule of POC in the pilot test area and the theoretical hypothesis model, the results indicate that the variation rule of the carbon number of the most abundant component in POC is the same, but the variation rule of light hydrocarbons and heavy hydrocarbons are different. The production monitoring data do not indicate the phenomenon of light hydrocarbons increase and the heavy hydrocarbons decrease when the oil in the flooding front is produced. The reason for this phenomenon may be that the flooding front is small and the sampling time interval is too long, resulting in failure to monitor the production data at this stage. At other production stages, the variation rule of POC in the pilot test area and the theoretical hypothesis model is the same. Therefore, it is considered that the variation rule of POC in the pilot test area is the same as the theoretical hypothesis model, and the correctness of the physical model is verified.

6 Conclusion

In this study, through analyzing the CO₂ flooding process in the low permeability reservoir at different inter-well reservoir characteristics, the physical model of POC variation was established, and the variation reason and rule were defined. Based on the experiments study of oil-CO₂ system properties and the precise experiments matching, the numerical model, including 34 components, was established, and simulated the POC variation rule during CO₂ flooding in low permeability reservoir at different inter-well reservoir characteristics. The POC monitoring data of CO₂ flooding pilot test area of low permeability reservoir in northeastern China were analyzed, and the POC variation rule during the oilfield production was obtained. Three conclusions can be drawn from this study.

First, the existence of the inter-well channeling-path and the difference of the permeability between matrix and channeling-path are the main reasons for the POC variation during CO₂ flooding in low permeability.

Second, for the low permeability reservoirs with homogeneous inter-well reservoir, the variation of the light hydrocarbon content in POC increase initially followed by a decrease, while the variation of the heavy hydrocarbon content in POC is completely opposite. The carbon number of the most abundant component in POC will gradually increase.

Third, for the low permeability reservoirs with the channeling-path existing in the inter-well reservoir, the variation rule of the light hydrocarbon content in POC is an increase-decrease-increase-decrease, while the variation rule of the heavy hydrocarbon content in POC is completely opposite. The variation rule of carbon number of the most abundant component in POC is an increase-decrease-increase.

Funding Statement: This work was supported by the National Key Research and Development Plan (No. 2018YFB0605500) and National Science and Technology Major Projects (No. 2017ZX05009004).

Conflicts of Interest: The authors declare that they have no conflicts of interest to report regarding the present study.

References

- Asif, M.; Muneer, T.** (2007): Energy supply, its demand and security issues for developed and emerging economies. *Renewable and Sustainable Energy Reviews*, vol. 11, no. 7, pp. 1388-1413. DOI 10.1016/j.rser.2005.12.004.
- Cao, M.; Gu, Y. A.** (2013): Physicochemical characterization of produced oils and gases in immiscible and miscible CO₂ flooding processes. *Energy & Fuels*, vol. 27, no. 1, pp. 440-453. DOI 10.1021/ef301407k.
- Darvish, G. R.; Lindeberg, E. G. B.; Holt, T.; Utne, S. A.; Kleppe, J.** (2006). Reservoir conditions laboratory experiments of CO₂ injection into fractured cores. *SPE/DOE Symposium on Improved Oil Recovery, Tulsa*.

Diwu, P. X.; Liu, T. J.; You, Z. J.; Hou, G. G.; Qiao, R. W. et al. (2018): Study on pulse characteristic of produced crude composition in CO₂ flooding pilot test. *Geofluids*, vol. 2018, pp. 1-5.

Dria, D. E.; Pope, G. A.; Sepehrnoori, K. (1993): Three-phase gas/oil/brine relative permeability measured under CO₂ flooding conditions. *SPE Reservoir Engineering*, vol. 8, no. 2, pp. 143-150. DOI 10.2118/20184-PA.

Gao, Y. C.; Zhao, M. F.; Wang, J. B.; Zong, C. (2014): Performance and gas breakthrough during CO₂ immiscible flooding in ultra-low permeability reservoirs. *Petroleum Exploration and Development*, vol. 41, no. 1, pp. 88-95. DOI 10.1016/S1876-3804(14)60010-0.

Grogan, A. T.; Pinczewski, W. V. (1987): The role of molecular diffusion processes in tertiary CO₂ flooding. *Journal of Petroleum Technology*, vol. 39, no. 5, pp. 591-602. DOI 10.2118/12706-PA.

Hamouda, A. A.; Chukwudeme, E. A.; Mirza, D. (2009): Investigating the effect of CO₂ flooding on asphaltenic oil recovery and reservoir wettability. *Energy & Fuels*, vol. 23, no. 2, pp. 1118-1127. DOI 10.1021/ef800894m.

Hu, W. R.; Wei, Y.; Bao, J. W. (2018): Development of the theory and technology for low permeability reservoirs in China. *Petroleum Exploration and Development*, vol. 45, no. 5, pp. 685-697. DOI 10.1016/S1876-3804(18)30072-7.

Holm, L. W. (1982): CO₂ flooding: its time has come. *Journal of Petroleum Technology*, vol. 34, no. 12, pp. 2739-2745. DOI 10.2118/11592-PA.

Hu, Y. L.; Hao, M. Q.; Chen, G. L.; Sun, R. Y.; Li, S. (2019): Technologies and practice of CO₂ flooding and sequestration in China. *Petroleum Exploration and Development*, vol. 46, no. 4, pp. 753-766. DOI 10.1016/S1876-3804(19)60233-8.

Li, M. T.; Shan, W. W.; Liu, X. G.; Shang, G. H. (2007): Laboratory study on miscible oil displacement mechanism. *Acta Petrolei Sinica*, vol. 27, no. 3, pp. 80-83.

Li, D. P. (1998). Main problems in developing low permeability reservoir and its improvement ways. *SPE International Oil and Gas Conference and Exhibition in China, Beijing, China*.

Liu, J. J.; Li, Q. S. (2012): Numerical simulation of injection water flow through mudstone interlayer in low permeability oil reservoir. *Disaster Advances*, vol. 5, no. 4, pp. 1639-1645.

Li, S. H.; Zhao, J. Y.; Cui, P. F.; Yang, J. L.; Chen, W. L. (2008): Strategies of development technology for ultra-low permeability reservoir. *Lithologic Reservoirs*, vol. 20, no. 3, pp. 128-131.

Ma, J. H.; Wang, X. Z.; Gao, R. M.; Zeng, F. H.; Huang, C. X. et al. (2016): Study of cyclic CO₂ injection for low-pressure light oil recovery under reservoir conditions. *Fuel*, vol. 174, pp. 296-306. DOI 10.1016/j.fuel.2016.02.017.

Orr, F. M.; Silva, M. K.; Lien, C. L.; Pelletier, M. T. (1982): Laboratory experiments to evaluate field prospects for CO₂ flooding. *Journal of Petroleum Technology*, vol. 34, no. 4, pp. 888-898. DOI 10.2118/9534-PA.

Qin, J. H.; Han, H. S.; Liu, X. L. (2015): Application and enlightenment of carbon dioxide flooding in the United States of America. *Petroleum Exploration and Development*, vol. 42, no. 2, pp. 232-240.

Ruan, M.; Wang, L. G. (2002): Low-permeability oilfield development and pressure-sensitive effect. *Acta Petrolei Sinica*, vol. 23, no. 3, pp. 73-76.

Shi, J. Q.; Xue, Z. Q.; Durucan, S. (2011): Supercritical CO₂ core flooding and imbibition in berea sandstone—CT imaging and numerical simulation. *Energy Procedia*, vol. 4, pp. 5001-5008. DOI 10.1016/j.egypro.2011.02.471.

Wang, T. R.; Zhang, Y.; Li, L.; Yang, Z.; Liu, Y. F. et al. (2018): Experimental study on pressure-decreasing performance and mechanism of nanoparticles in low permeability reservoir. *Journal of Petroleum Science and Engineering*, vol. 160, pp. 693-703. DOI 10.1016/j.petrol.2018.03.070.

Wang, H.; Liao, X. W.; Zhao, X. L. (2014): The influence of CO₂ solubility in reservoir water on CO₂ flooding and storage of CO₂ injection into a water flooded low permeability reservoir. *Energy Sources Part A: Recovery Utilization and Environmental Effects*, vol. 36, no. 8, pp. 815-821. DOI 10.1080/15567036.2012.741654.

Wang, H. X.; Wang, G.; Chen, Z. X.; Wong, R. C. K. (2010): Deformational characteristics of rock in low permeable reservoir and their effect on permeability. *Journal of Petroleum Science and Engineering*, vol. 75, no. 1, pp. 240-243. DOI 10.1016/j.petrol.2010.11.015.

Xiao, P. F.; Yang, Z. M.; Wang, X. W.; Xiao, H. M.; Wang, X. Y. (2016): Experimental investigation on CO₂ injection in the Daqing extra/ultra-low permeability reservoir. *Journal of Petroleum Science and Engineering*, vol. 149, pp. 765-771. DOI 10.1016/j.petrol.2016.11.020.

Zhou, T.; Liu, X. W.; Yang, Z. M.; Li, X. Z.; Wang, S. Y. (2015): Experimental analysis on reservoir blockage mechanism for CO₂ flooding. *Petroleum Exploration and Development*, vol. 42, no. 4, pp. 502-506.